

IC 4663: the first unambiguous [WN] Wolf–Rayet central star of a planetary nebula[★]

B. Miszalski,^{1,2†} P. A. Crowther,³ O. De Marco,⁴ J. Köppen,⁵ A. F. J. Moffat,^{6,7}
A. Acker⁵ and T. C. Hillwig⁸

¹South African Astronomical Observatory, PO Box 9, Observatory 7935, South Africa

²Southern African Large Telescope Foundation, PO Box 9, Observatory 7935, South Africa

³Department of Physics and Astronomy, University of Sheffield, Hounsfield Road, Sheffield S3 7RH

⁴Department of Physics and Astronomy, Macquarie University, Sydney, NSW 2109, Australia

⁵Observatoire astronomique de Strasbourg, Université de Strasbourg, CNRS, UMR 7550, 11 rue de l'Université, F-67000 Strasbourg, France

⁶Dépt. de physique, Univ. de Montréal CP 6128, Succ. Centre-Ville, Montréal, QC H3C 3J7, Canada

⁷Centre de recherche en astrophysique du Québec, Canada

⁸Department of Physics and Astronomy, Valparaiso University, Valparaiso, IN 46383, USA

Accepted 2012 March 14. Received 2012 March 2; in original form 2012 February 3

ABSTRACT

We report on the serendipitous discovery of the first central star of a planetary nebula (PN) that mimics the helium- and nitrogen-rich WN sequence of massive Wolf–Rayet (WR) stars. The central star of IC 4663 (PN G346.2–08.2) is dominated by broad He II and N V emission lines which correspond to a [WN3] spectral type. Unlike previous [WN] candidates, the surrounding nebula is unambiguously a PN. At an assumed distance of 3.5 kpc, corresponding to a stellar luminosity of $4000 L_{\odot}$, the $V = 16.9$ mag central star remains 4–6 mag fainter than the average luminosity of massive WN3 stars even out to an improbable $d = 8$ kpc. The nebula is typical of PNe with an elliptical morphology, a newly discovered asymptotic giant branch (AGB) halo, a relatively low expansion velocity ($v_{\text{exp}} = 30 \text{ km s}^{-1}$) and a highly ionized spectrum with an approximately solar chemical abundance pattern. The [WN3] star is hot enough to show Ne VII emission ($T_* = 140 \pm 20 \text{ kK}$) and exhibits a fast wind ($v_{\infty} = 1900 \text{ km s}^{-1}$), which at $d = 3.5$ kpc would yield a clumped mass-loss rate of $\dot{M} = 1.8 \times 10^{-8} M_{\odot} \text{ yr}^{-1}$ with a small stellar radius ($R_* = 0.11 R_{\odot}$). Its atmosphere consists of helium (95 per cent), hydrogen (<2 per cent), nitrogen (0.8 per cent), neon (0.2 per cent) and oxygen (0.05 per cent) by mass. Such an unusual helium-dominated composition cannot be produced by any extant scenario used to explain the H-deficiency of post-AGB stars. The O(He) central stars share a similar composition and the discovery of IC 4663 provides the first evidence for a second He-rich/H-deficient post-AGB evolutionary sequence [WN] \rightarrow O(He). This suggests that there is an alternative mechanism responsible for producing the majority of H-deficient post-AGB stars that may possibly be expanded to include other He-rich/H-deficient stars such as R Coronae Borealis stars and AM Canum Venaticorum stars. The origin of the unusual composition of [WN] and O(He) central stars remains unexplained.

Key words: stars: abundances – stars: AGB and post-AGB – stars: mass-loss – stars: Wolf–Rayet – planetary nebulae: general – planetary nebulae: individual: PN G346.2–08.2.

1 INTRODUCTION

Planetary nebulae (PNe) are the result of low–intermediate mass stars ($\sim 1\text{--}8 M_{\odot}$) that have experienced heavy mass loss during the asymptotic giant branch (AGB) phase. Their gaseous envelopes are ionized by hot pre-white dwarfs (WDs) ($T_{\text{eff}} \sim 30\text{--}140 \text{ kK}$) whose diverse spectroscopic appearance (Méndez 1991) reflects different

[★]Based on observations made with Gemini South under programme GS-2011A-Q-65 (PI: B. Miszalski).
[†]E-mail: brent@saao.ac.za

wind properties and atmospheric compositions. A subset of central stars have H-deficient atmospheres composed primarily of helium, carbon and oxygen with fast and dense winds that produce broad emission lines. Their spectroscopic appearance mimics the carbon sequence of massive Wolf-Rayet (WR) stars and they are classified into either [WO] or [WC] types, the brackets distinguishing them apart from massive stars (van der Hucht 2001), depending on which emission lines are present and their relative intensities (Crowther, De Marco & Barlow 1998; Acker & Neiner 2003). Despite recent surveys that have dramatically increased the number of central stars that belong to the [WC] sequence (Acker & Neiner 2003; Górny et al. 2004, 2009, 2010; DePew et al. 2011), their origin and evolution remain poorly understood.

Werner & Herwig (2006) reviewed possible scenarios that may explain the H-deficiency of [WC] central stars¹ and their progeny the PG 1159 stars (Wesemael, Green & Liebert 1985). After the central star has left the AGB phase a late thermal pulse (LTP) or very late thermal pulse (VLTP) would reignite helium-shell burning (e.g. Blöcker 2001; Herwig 2001). The star is sent back to the AGB phase, i.e. it becomes ‘born-again’ (Schönberner 1979), and any residual hydrogen is either burned or diluted below the observable detection limit. The AGB final thermal pulse (AFTP) variant may also be invoked to explain some instances where a small amount of observable hydrogen remains. At this point the star enters the [WC] sequence with an H-deficient atmosphere mostly made of helium (~30–50 per cent), carbon (~30–60 per cent) and oxygen (~2–20 per cent).

A post-AGB H-deficient evolutionary sequence [WCL] → [WCE] → PG 1159 has been proposed in which late-type [WC] central stars evolve into early-type [WC] and [WO] central stars, followed by PG 1159 stars which appear preferentially in the oldest PNe (Napiwotzki & Schönberner 1995) and in isolation once the surrounding PNe have dissipated into the interstellar medium (ISM).² Unless there is a residual amount of hydrogen the end product will be a non-DA WD. This evolutionary sequence is supported by the strong similarities in derived atmospheric compositions (Werner & Herwig 2006) and some transition objects (e.g. Bond 2008). A key question is whether the H-deficiency of all members of the sequence can be explained by the LTP, VLTP and AFTP scenarios. Górny & Tylenda (2000) found the evolutionary status of nebulae surrounding H-deficient central stars to be consistent with H-rich central stars, rather than following the paths predicted by LTP or VLTP scenarios. It is therefore debatable whether the few documented LTP and VLTP events (Schönberner 2008) mandate the same origin for the larger population of H-deficient central stars. Indeed, there may even be an alternative common-envelope (CE) (De Marco & Soker 2002; De Marco 2008; Hajduk, Zijlstra & Gesicki 2010) or nova-like explanation for such objects (Wesson, Liu & Barlow 2003; Wesson et al. 2008; Lau, De Marco & Liu 2011).

Even more difficult to explain are the helium-rich H-deficient stars which do not fit the carbon-rich post-AGB H-deficient sequence. These include four O(He) stars (Rauch, Dreizler & Wolff 1998), two of which are central stars of PNe (Rauch, Köppen &

Werner 1994, 1996), R Coronae Borealis (RCB) stars (Clayton 1996), extreme helium B stars and helium-rich subdwarf O stars (see e.g. Werner & Herwig 2006). With typical helium mass fractions $\gtrsim 90$ per cent and trace amounts of other elements the chemical compositions of these stars have never been predicted by the born-again scenarios, i.e. they simply should not exist! On the whole these stars are scarce compared to the carbon-rich sequence and probably form a second, parallel post-AGB H-deficient sequence. Evidence for such a sequence is tentative however, based primarily on their common composition rather than other evolutionary ties. It has been suggested that RCB stars are the progenitors of O(He) stars, although the circumstances of this possible connection remain unclear. After the discovery of a low $^{16}\text{O}/^{18}\text{O}$ ratio by Clayton et al. (2007) strongly pointing to a merger origin for RCB stars, an end to the protracted debate on the formation of RCB stars seemed to be in sight. However, not only is the RCB evolutionary path complicated by a connection with [WC] central stars (Clayton & De Marco 1997; Clayton et al. 2006; Clayton et al. 2011a), but there are indications of a mixed origin within the RCB class itself (Clayton et al. 2011b).

It is imperative that more members of the He-rich/H-deficient class are found and studied to establish a second evolutionary sequence. If this can be achieved, then there should exist another mechanism responsible for H-deficiency, one which may also help explain the origin of the carbon-rich sequence. A long sought after solution may be [WN] type WR central stars that mimic the helium- and nitrogen-rich WN sequence in massive stars (Smith, Shara & Moffat 1996). Although some candidates have been proposed, none have turned out to be satisfactory and the existence of the class remains unproven.

Here we report on the serendipitous discovery of a [WN] central star in the PN IC 4663 (PN G346.2–08.2; Fleming & Pickering 1910). Observations of IC 4663 were made during the Gemini South programme GS-2011A-Q-65 (PI: B. Miszalski) which aimed to discover new close binary central stars of PNe via radial-velocity (RV) variability (e.g. Miszalski et al. 2011a). Programme targets were selected based on the nebula trends identified by Miszalski et al. (2009b) to be provisionally associated with binarity that includes bipolar nebulae, nebulae with collimated outflows (jets) and low-ionization structures (e.g. Gonçalves, Corradi & Mampaso 2001). As noted by Miszalski et al. (2009b), a large number of PNe with WR central stars overlap with this morphological prescription and so it was not unexpected that new examples would be found during the programme.

This paper is structured as follows. Section 2 reviews previous [WN] candidates. Section 3 describes Gemini South spectroscopy and atmospheric modelling of the previously unobserved central star of IC 4663. The basic nebula properties and chemical abundances are presented in Section 4. Section 5 establishes the [WN] nature of the central star by proving the bona fide PN nature of IC 4663 and introduces the second post-AGB H-deficient evolutionary sequence. We conclude in Section 6.

2 PREVIOUS [WN] CANDIDATES

Around 8 per cent of massive Galactic WN stars are known to have surrounding nebulae (Stock & Barlow 2010). Until improved observations could reliably determine the luminosity of their central stars, some of these nebulae were misclassified as PNe. As the distances to PNe are extremely difficult to estimate, this has not helped clarify the status of many candidates. Fig. 1 shows M 1-67 which was included in the PN catalogue of Perek & Kohoutek (1967); however, its WN8h star WR 124 was only later proven

¹ Massive WC stars are extremely H-deficient, but for a different reason. A strong wind has peeled off the outer H-containing layers exposing in turn the C- and O-rich products of triple- α He burning.

² This differs from massive WC stars which appear to have their subtype determined by their initial metallicity, although some evolution from late to early may also occur (Smith & Maeder 1991).

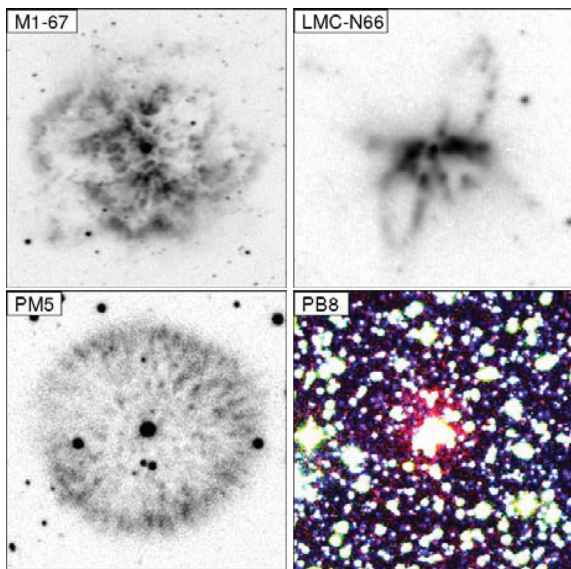


Figure 1. A selection of previous [WN] candidates. The M 1-67 (Drew et al. 2005; González-Solares et al. 2008) and PM 5 (see text) images were both taken with an $H\alpha+[N\text{ II}]$ filter, while LMC-N66 was observed with the clear filter of *HST* STIS. The colour-composite image of PB 8 is made from SHS $H\alpha+[N\text{ II}]$ (red), SHS short-red (green) and SuperCOSMOS Sky Survey B_J (blue; Hambly et al. 2001). It reveals for the first time a faint AGB halo with a diameter up to ~ 80 arcsec surrounding PB 8 (the bright central source). Image dimensions are 120×120 arcsec² (M 1-67), 6×6 arcsec² (LMC-N66), 40×40 arcsec² (PM 5) and 4×4 arcmin² (PB 8). In all cases north is up and east is to the left.

to be a massive star by Crawford & Barlow (1991a) based on the kinematic distance measured from the interstellar Na I D_2 absorption line.³ The flocculent appearance of the nebula, evident in Fig. 1, but best seen in *HST* observations (Grosdidier et al. 2001a), also bears more resemblance to nebulae around massive WN stars including RCW 58 around WR 40 (Chu 1982) and NGC 6888 around WR 136 (Wendker et al. 1975). Another similar case to M 1-67 is We 21 (Duerbeck & Reipurth 1990) which was proven to host a massive star by Crawford & Barlow (1991b).

Other [WN] candidates have proven very difficult to establish as promising candidates for clear-cut low-mass analogues of the massive WN sequence. The most extensively studied is LMC-N66 in the Large Magellanic Cloud (see e.g. Peña et al. 1994, 1997, 2004, 2008; Hamann et al. 2003). Multiple outbursts have been recorded in the central star which shows a mid-WN spectral type during outburst. Peña et al. (2004) studied the surrounding nebula (Fig. 1) which resembles point-symmetric PNe in the Milky Way (e.g. Fleming 1; Lopez, Meaburn & Palmer (1993) and shows multiple emission components that span $130\text{--}160$ km s⁻¹. The luminosity spans $\log L/L_{\odot} = 4.6\text{--}5.4$ (Hamann et al. 2003), too high to be consistent with a typical PN central star. Hamann et al. (2003) presented a number of possible explanatory scenarios, none of which is without difficulty, although a massive star in a CE phase with a low-mass companion or a massive WD accreting matter in a close binary seem to be preferred. Binary stellar evolution is therefore likely responsible for the WN features of LMC-N66, as is similarly seen in

symbiotic novae such as RR Tel and PU Vul (Thackeray & Webster 1974; Nussbaumer 1996).

Morgan, Parker & Cohen (2003) discovered a WN6 star in the nebula PM 5 and argued for a PN status based on the nebula density, size, ionized mass, morphology, near-infrared and mid-infrared properties mostly being similar to PNe. A non-PN status is supported by the anomalously high expansion velocity (165 km s⁻¹), low Galactic latitude ($b = +0^{\circ}.69$), high reddening [$E(B - V) = 3.0\text{--}3.5$ mag] and the analysis by Todt et al. (2010b). Furthermore, Fig. 1 shows a previously unpublished Very Large Telescope (VLT) FORS2 (Appenzeller et al. 1998) image observed under European Southern Observatory (ESO) programme ID 077.B-0430(B) (PI: M. Peña). The 20-s image taken through the $H\alpha+83$ filter [central wavelength (λ_{cen}) and full width at half-maximum (FWHM) of 656.3 and 6.1 nm, respectively] reveals a flocculent appearance which was not visible in the lower resolution SuperCOSMOS $H\alpha$ Survey (SHS) discovery images (Parker et al. 2005). Similarly, the WN6 central star of A48 (Abell 1966; Wachter et al. 2010; DePew et al. 2011) is also likely to be a massive star; however, this object has not yet been studied in detail. It is also located at a low Galactic latitude ($b = +0^{\circ}.4$), has a double-ring morphology (Stock & Barlow 2010) and is also quite reddened [$E(B - V) = 2.0$ mag; DePew et al. 2011].

Several other candidates have also been identified based on the presence of weak nitrogen emission features in addition to their [WO/WC] spectra. The [WO4/WC4] central stars of NGC 6751 (Aller 1968; Koesterke & Hamann 1997), PMR1 and PM3 (Morgan, Parker & Russeil 2001; Parker & Morgan 2003) exhibit weak $N\text{ IV}$ and $N\text{ V}$ emission features. Further examples are evident amongst the [WO4pec] and [WO] central stars studied by Acker & Neiner (2003). In the case of NGC 6751 nitrogen accounts for no more than 1 per cent by mass in an otherwise typical [WO/WC] atmospheric composition of 55 per cent helium, 30 per cent carbon and 15 per cent oxygen (Koesterke & Hamann 1997). Others were analysed by Todt et al. (2008) who found that nitrogen contributed no more than 1–2 per cent by mass.

Todt et al. (2010a,b) found the central star of PB 8 to show clear nitrogen emission features and determined a nitrogen mass fraction of 2 per cent. Its overall atmospheric composition was found to be made of oxygen and carbon each 1.3 per cent by mass, helium 55 per cent and hydrogen an unusually high 40 per cent. This is most unlike [WO/WC] central stars which have significantly higher fractions of carbon and oxygen (Crowther 2008). The PN nature of PB 8 is demonstrated by its relatively low expansion velocity (19 ± 6 km s⁻¹) and especially our discovery in Fig. 1 of a faint AGB halo (Corradi et al. 2003). Todt et al. (2010a) proposed that PB 8 belongs to a [WN/WC] classification, an analogue of the massive WN/WC stars (e.g. Massey & Grove 1989; Crowther, Smith & Willis 1995b) which account for <5 per cent of massive WR stars (van der Hucht 2001). Therefore, strictly speaking, PB 8 is not a true [WN] nucleus due to the additional [WC] features.

To summarize, no [WN] candidate has been unambiguously proven to be surrounded by a PN. While PB 8 is certainly a PN, it appears to be a [WN/WC] hybrid rather than a strict [WN].

3 THE CENTRAL STAR

3.1 Observations

We used the Gemini Multi-Object Spectrograph (GMOS; Hook et al. 2004) on Gemini South to obtain three spectra of the central star of IC 4663 on 2011 June 27, July 2 and July 3 as part of the

³ Marchenko, Moffat & Crowther (2010) recently confirmed this result by analysing the nebula expansion parallax with two-epoch *HST* observations.

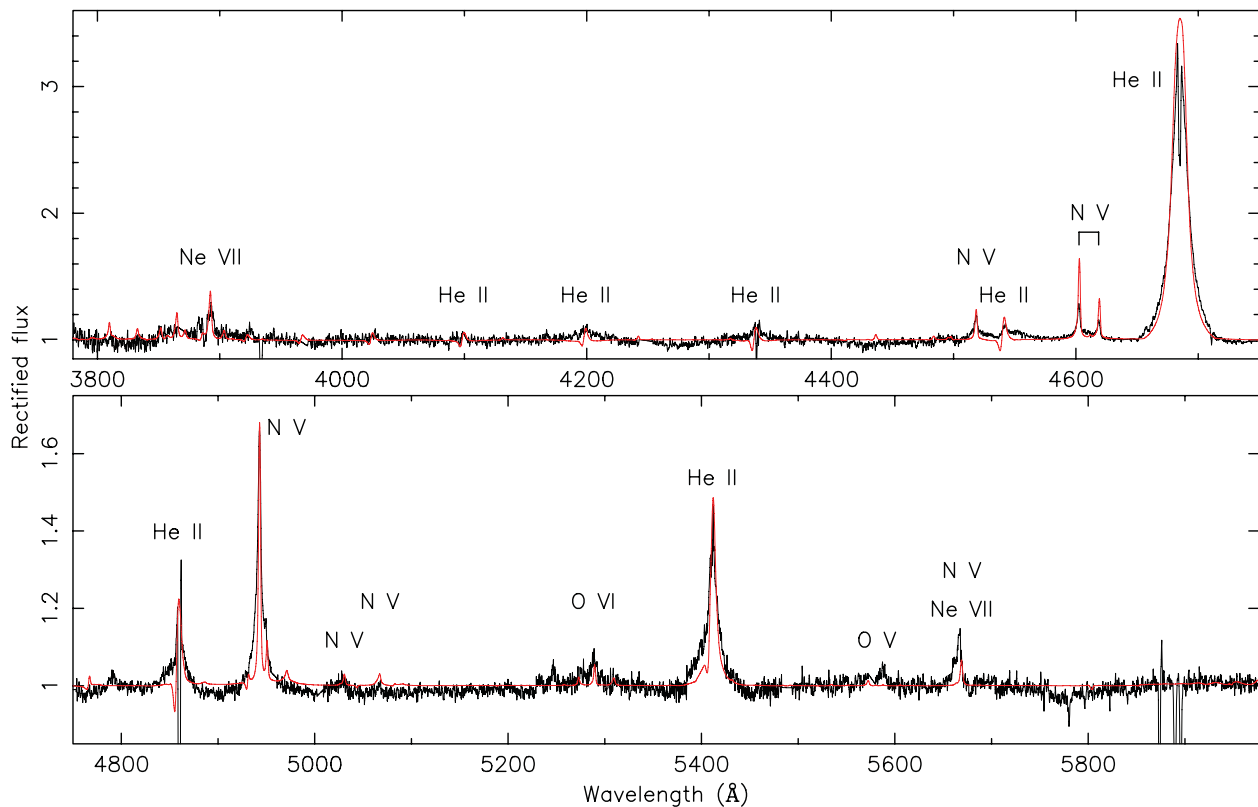


Figure 2. Rectified Gemini South GMOS spectrum of the central star of IC 4663 (black) with the CMFGEN NLTE model (red, see Section 3.3). The main emission lines are identified, most belonging to He II and N V, which, together with the absence of C IV and He I emission, indicate a [WN3] spectral type. The apparent double-peaked profile of He II λ 4686 is an artefact of nebula subtraction and does not influence the NLTE analysis.

GS-2011A-Q-65 programme (PI: B. Miszalski). The B1200 grating was used with a 0.75-arcsec slit oriented at a position angle of 90° to provide wavelength coverage from 3767 to 5228 Å (June 27 and July 3) and 4507 to 5977 Å (July 2) at 1.6 Å resolution (FWHM) with a reciprocal dispersion of $0.23 \text{ \AA pixel}^{-1}$ (1×2 binning in dispersion and spatial axes, respectively). The science exposure times were 1800 s (June 27) and 2400 s (July 2 and 3) and were accompanied by contemporaneous arc lamp exposures. The data were reduced with the Gemini IRAF package after which nebula-subtracted one-dimensional spectra were extracted using the APALL IRAF task. A non-uniform spatial profile in the nebula emission lines produced a small amount of oversubtraction at the Balmer lines, He II λ 4686, 5412 and He I λ 5876. The one-dimensional spectra were flux calibrated with a spectrum of the spectrophotometric standard star EG 274 in the usual fashion.

The V magnitude of the central star is not well determined in the literature with discordant estimates of $V = 15.16^{+0.29}_{-0.23}$ mag (Shaw & Kaler 1989) and $B = 18.0 \pm (0.5-1.0)$ mag (Tylenda et al. 1991). We retrieved the processed and combined *HST* $F555W$ image (approx. Johnson V) of total duration 1020 s from the Hubble Legacy Archive⁴ (HLA) and performed aperture photometry on the central star following the Wide Field Planetary Camera 2 (WFPC2) Photometry Cookbook.⁵ Assuming $V - F555W = 0.05$ mag, suitable for an O5V star, we found $V = 16.90 \pm 0.05$ mag and fixed the ab-

solute flux scale of our GMOS spectrum to match the corresponding Vega flux at λ 5480 Å.

3.2 Spectral features and [WN3] classification

Fig. 2 shows the two 2400 s exposures averaged to achieve a signal-to-noise ratio (S/N) of at least ~ 60 in the continuum (except for $\lambda \leq 4500 \text{ \AA}$ where $S/N \gtrsim 30$) and rectified for comparison with the non-local thermodynamic equilibrium (NLTE) model described in Section 3.3. The spectrum is dominated by He II and N V emission lines typical of early-type WN stars (Crowther, Smith & Hillier 1995a) and shares the triangular line profiles of Galactic early-type WN stars (Smith et al. 1996). The Ne VII emission lines (Werner, Rauch & Kruk 2007) were never before seen in massive WN stars, whereas the weak O V and O VI emission lines are uncommon (e.g. the WN3pec star WR 46 shows relatively strong O VI λ 3811–3834; Crowther et al. 1995a). The high-S/N spectrum rules out the presence of He I and C IV emission lines which, combined with the already mentioned features, corresponds to a clear WN3 subtype (Smith et al. 1996). The WN3 subtype is not common amongst massive Galactic WN stars where only a few examples are known (e.g. Crowther et al. 1995a; Hamann, Koesterke & Wessolowski 1995; Smith et al. 1996). The equivalent width of He II λ 4686 ($\sim 40 \text{ \AA}$) is comparable to massive WN3 stars, whereas its FWHM is slightly lower than WN3 stars ($\sim 18.5 \text{ \AA}$). This behaviour is also seen in C III λ 5696 in the comparison between the [WC9] central star of BD+30 3639 and massive WC9 stars (Crowther, Morris & Smith 2006). In the rest of this paper we denote the classification as [WN3]

⁴ <http://hla.stsci.edu>

⁵ http://www.stsci.edu/hst/wfpc2/analysis/wfpc2_cookbook.html

to indicate that it is a bona fide central star of a PN (later proven in Section 5.1).⁶

3.3 NLTE modelling

We have analysed the GMOS spectrum of IC 4663 using CMFGEN (Hillier & Miller 1998) which solves the radiative transfer equation in the comoving frame subject to statistical and radiative equilibrium, assuming an expanding, spherically symmetric, homogeneous atmosphere, allowing for metal-line blanketing and wind clumping.

Our adopted model atom includes H I, He I–II, C IV, N IV–V, O IV–VI, Ne III–VIII, Si IV and Fe V–IX. In total 512 superlevels, 1907 levels and 28 397 NLTE transitions are simultaneously considered, with H/He, C/He, N/He, O/He variable, and Si and Fe mass fractions fixed at solar values (Asplund et al. 2009). We adopt a Ne mass fraction of 0.2 per cent, based on a number ratio of Ne/O = 0.25 from Wang & Liu (2008), and the solar O mass fraction of 0.55 per cent (Asplund et al. 2009).

In view of the relatively weak emission-line spectrum of IC 4663, the supersonic velocity law, $v_\infty(1 - R/r)^\beta$, is merged with a subsonic structure calculated using the NLTE plane-parallel code TLUSTY (Hubeny & Lanz 1995).⁷ In order to reproduce the morphology of He II $\lambda 4686$ we obtain $v_\infty = 1900 \text{ km s}^{-1}$ and $\beta \sim 2.5$, the former being similar to $v_\infty = 2000 \text{ km s}^{-1}$ as measured for the massive WN3 star WR 152 (Crowther et al. 1995a). A clumped mass-loss rate is calculated for an adopted volume filling factor of $f = 0.1$, although this is poorly constrained for IC 4663. While β values close to unity are normally found in weak-wind OB stars, larger values implying more extended accelerating zones are found in massive WR stars (e.g. Moffat 1996; Lépine & Moffat 1999).

Diagnostic optical lines of He II $\lambda 4686$ and Ne VII $\lambda 3890$ enable the stellar temperature of $T_* = 140 \pm 20 \text{ kK}$ to be obtained. Beyond this range, Ne VII weakens at higher temperatures, where it is replaced by Ne VIII (e.g. $\lambda 4340$), and at lower temperatures, where Ne VI strengthens (e.g. $\lambda 4973$). High lying recombination lines of N V ($\lambda\lambda 4945$) and O VI ($\lambda 5290$) serve as reliable N/He and O/He abundance diagnostics, from which mass fractions of 0.8 and 0.05 per cent are obtained, respectively. Negligible hydrogen is required to reproduce the lower members of the Pickering–Balmer series, He II $\lambda 5412$, He II+H β and He II $\lambda 4542$, permitting an upper limit of ~ 2 per cent by mass. Since there were no suitable diagnostics for C/He, we investigated whether we could place limits on the carbon mass fraction by recalculating the CMFGEN model with an elevated carbon abundance. The C IV $\lambda\lambda 5801, 5812$ emission lines became visible for values in excess of 0.1 per cent.

The CMFGEN model provides a satisfactory fit to the GMOS spectrum (Fig. 2), although O V $\lambda 5590$ is too weak, as is the blend of Ne VIII $\lambda 5668$ and N V $\lambda 5670$. In addition, higher members of the He II Pickering series are predicted to exhibit weak P Cygni profiles, in contrast to observations. The theoretical spectral energy distribution (SED) was matched to the dereddened GMOS spectrophotometry enabling a determination of luminosity and mass-loss rate. We obtained an interstellar extinction of $E(B - V) = 0.35 \pm 0.05$

⁶ Despite the good match with WN3 stars, we caution that the Smith et al. (1996) scheme was solely devised for massive WN stars. If a sufficient sample of [WN] stars were to be found, then a unified classification scheme may be required (e.g. Crowther et al. 1998) which may not necessarily match the existing one.

⁷ For our derived $T_* = 140 \text{ kK}$ and $\log L/L_\odot = 3.6$, we adopt $M = 0.6 M_\odot$ resulting in $\log g = 6.1$ for the TLUSTY model structure.

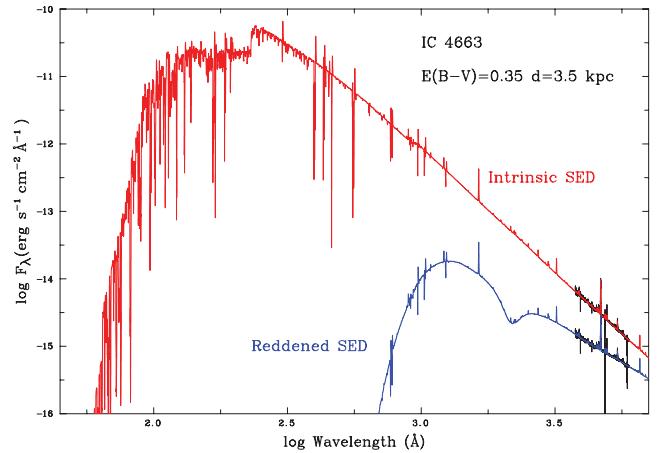


Figure 3. Intrinsic and reddened SEDs of the NLTE model (red and blue, respectively) with the GMOS spectrum (black).

($A_V = 1.1 \text{ mag}$) using a standard Galactic extinction law (Howarth 1983). This agrees well with the value of $E(B - V) = 0.4 \pm 0.1 \text{ mag}$ that Cavichia, Costa & Maciel (2010, hereafter CCM10) measured from the Balmer decrement of the surrounding nebula.

We adopt a distance of 3.5 kpc from the statistical Shklovsky distance scale of Stanghellini, Shaw & Villaver (2008, hereafter SSV08) which includes Magellanic Cloud PNe as calibrators. No individual error was given for the distance to IC 4663. We therefore take a conservative approach and assume a 2σ uncertainty of 60 per cent, which results in a distance of $3.5 \pm 2.1 \text{ kpc}$. With this distance an absolute magnitude of $M_V = +3.1 \text{ mag}$ is derived for the [WN3] central star of IC 4663. The bolometric correction for our CMFGEN model is -7.4 , resulting in $M_{\text{Bol}} = -4.3$ or $\log L/L_\odot = 3.6$. For this luminosity, a stellar radius of $R_* = 0.11 R_\odot$ and a clumped mass-loss rate of $\dot{M} = 1.8 \times 10^{-8} M_\odot \text{ yr}^{-1}$ are required. As indicated in Fig. 3, the SED of IC 4663 is exceptionally hard, with $Q_0 = 10^{47.39} \text{ s}^{-1}$, $Q_1 = 10^{47.27} \text{ s}^{-1}$ and $Q_2 = 10^{46.47} \text{ s}^{-1}$ for the H I, He I and He II continua, respectively. Table 1 summarizes the stellar parameters of the [WN3] central star and includes ranges of distance-dependent quantities for the 2.1-kpc uncertainty in the distance.

Table 1. Stellar parameters of the [WN3] central star of IC 4663. Quantities in square brackets represent the range of parameter values for the 2.1 kpc uncertainty in distance.

T_*	140 ± 20	kK
$\log g$	6.1	(assuming $M = 0.6 M_\odot$)
v_∞	1900	km s^{-1}
$E(B - V)$	0.35 ± 0.05	mag
V	16.90 ± 0.05	mag
d	3.5 ± 2.1	kpc (SSV08)
M_V	3.1	mag [2.1–5.1]
$\log L/L_\odot$	3.6	[2.8–4.0]
R_*	0.11	R_\odot [0.04–0.17]
\dot{M}	1.8	$10^{-8} M_\odot \text{ yr}^{-1}$ [0.5–3.5]
H	<2	mass fraction (per cent)
He	95	mass fraction (per cent)
C	<0.1	assumed mass fraction (per cent)
N	0.8	mass fraction (per cent)
O	0.05	mass fraction (per cent)
Ne	0.2	mass fraction (per cent)

Table 2. Stellar properties and transformed radii R_t for three massive WN3 stars (Hamann et al. 2006) and the [WN3] central star of IC 4663. The D quantity is the wind clumping factor.

Object	R_*/R_\odot	$\log L/L_\odot$	v_∞	$\log \dot{M}$	D	R_t/R_\odot
WR3	2.65	5.6	2700	-5.3	4	15.1
WR 46	2.11	5.8	2300	-5.1	4	6.8
WR 152	2.20	5.3	2000	-5.5	4	11.9
IC 4663	0.11	3.6	1900	-7.7	10	13.4

With the derived stellar properties of IC 4663 we can quantitatively judge its wind strength against massive WN3 stars. Table 2 summarizes the stellar properties of massive WN3 stars (Hamann, Gräfener & Liermann 2006) and IC 4663, together with the transformed radius R_t (see equation 1 of Hamann et al. 2006). The magnitude of R_t diagnoses the wind density (i.e. the emission-line strength) which is essentially the same for massive WR and [WR] stars of a given spectral type, despite the order-of-magnitude difference in radii (e.g. Crowther et al. 2006). Low values of R_t correspond to strong, thick winds and high values to weak, thin winds. Since the R_t of IC 4663 lies between WR 152 and WR3, the stellar wind is similarly dense to massive WN3 stars, entirely consistent with our morphological [WN3] classification. This argues against any weak-wind classification of the central star of IC 4663 [e.g. Of or Of-WR; see Méndez, Herrero & Manchado (1990) and Méndez (1991)].

3.4 Variability

The GMOS observations were taken on three separate epochs, namely $E1$ (June 27), $E2$ (July 2) and $E3$ (July 3), separated by $E2 - E1 = 5.273$ d, $E3 - E2 = 1.005$ d and $E3 - E1 = 6.278$ d. Fig. 4 depicts the narrow N v emission lines which show a root mean square RV variability of 3–4 km s⁻¹ using cross-correlation techniques, i.e. no evidence of variability $\gtrsim 5$ –10 km s⁻¹. A main-sequence or WD companion in a post-CE binary (i.e. $P \lesssim 1$ d) would produce larger variability than our detection limit and is therefore unlikely to be present unless the orbital inclination is very

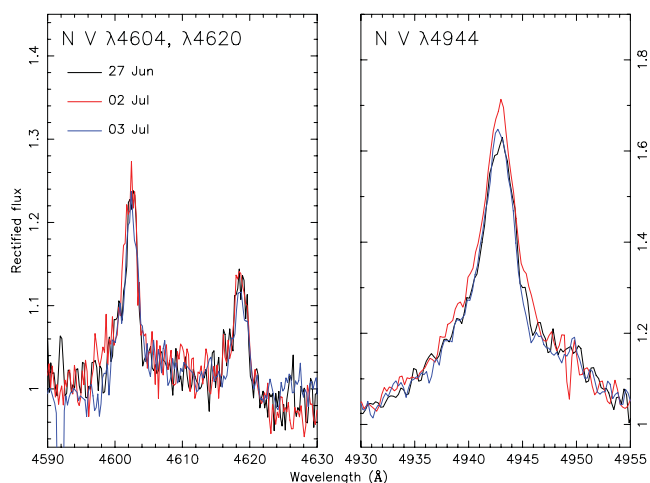


Figure 4. Line profiles of N v $\lambda\lambda 4604$, 4620 and 4944 in the overlap region between all three epochs. Note the absence of any RV shifts $\gtrsim 5$ –10 km s⁻¹ that argues against the presence of a post-common-envelope binary companion.

low. The lack of temporal coverage less than a day also makes this possibility difficult to rule out entirely since the median period of close binary central stars is 0.3–0.4 days (Miszalski et al. 2009a, 2011b). The small variability in the line intensity profile may be explained by either noise in the spectrum or wind turbulence (e.g. Grosdidier, Acker & Moffat 2000, 2001b). There is little historical information on any photometric variability of IC 4663, e.g. whether an LMC-N66-like outburst has occurred. The insensitivity of Shaw & Kaler (1989) to magnitudes fainter than $V = 16$ provides a reasonable lower limit to the central star magnitude in 1989. The very bright nebula precludes measuring central star magnitudes from photographic plate material.

4 THE NEBULA

4.1 Observations and basic properties

The nebulae surrounding WR central stars contain valuable additional information to better understand the nature of their nuclei. Acquisition images of IC 4663 were taken during our GMOS programme through the filters Ha (120 s), OIII (120 s) and OIIIC (90 s), whose central wavelengths/FWHMs are 656.0/7.2 nm, 499.0/4.5 nm and 514.0/8.8 nm, respectively. The seeing was 1.5 arcsec (FWHM) on June 27 and 1.1 arcsec (FWHM) on July 2 and 3 as measured from the OIIIC images.

Fig. 5 shows the GMOS [O III] image overlaid with a colour-composite image made from the *HST* images published by Hajian et al. (2007). Revealed for the first time is a low surface brightness AGB halo (Corradi et al. 2003). A brightened rim lies 22 arcsec SE of the central star and is likely caused by ISM interaction. At ~ 0.25 per cent of the main nebula peak [O III] intensity, i.e. 400 times fainter, roughly corresponding to the extent visible in the scaling selected for Fig. 5, the halo measures 52.5×55.0 arcsec² across. The halo may even reach as far as 72 arcsec across before it becomes indistinguishable from the sky background.

The PN morphology is best captured by the aforementioned Hajian et al. (2007) *HST* images that were taken on 1998 August 4 through the *F502N* ([O III]), *F658N* ([N II]) and *F555W* filters. The data were retrieved from the HLA and have total exposure times of 520, 320 and 1020 s, respectively. A nebula diameter of 16.0×19.5 arcsec² was measured at 10 per cent of peak intensity in the *F502N* image. The overall morphology appears to be an ellipsoidal bubble surrounded by a second fainter shell similar to other bright PNe (e.g. NGC 1501). This interpretation is consistent with the high-resolution spectrograms published by Hajian et al. (2007). As previously mentioned, low-ionization filaments are also present (Gonçalves et al. 2001; visible as red filaments in Fig. 5) and were part of the selection criteria for the inclusion of this PN in our GMOS programme.

Combining the equatorial expansion velocity of 30 km s⁻¹ measured by Hajian et al. (2007), with the minor axis nebula diameter of 16 arcsec and our assumed distance of 3.5 kpc (SSV08), gives an expansion age of $t_{\text{neb}} \sim 4400$ years. For the halo we assume a 15 km s⁻¹ expansion velocity (Corradi et al. 2003) to find $t_{\text{halo}} \sim 30500$ years and $t_{\text{halo}} - t_{\text{neb}} \sim 26000$ years. We derive a heliocentric RV v_{hrv} of -78 ± 3 km s⁻¹ from the brightest emission lines in the GMOS nebula spectra. This value is in agreement with -74 km s⁻¹ measured by Beaulieu, Dopita & Freeman (1999). Shaw & Kaler (1989) measured integrated fluxes for the nebula and found $\log F(\text{H}\beta) = -11.44$ (-10.93 dereddened), where $F(\text{H}\beta)$ is in units of erg cm⁻² s⁻¹. Table 3 summarizes the basic observed properties of IC 4663.

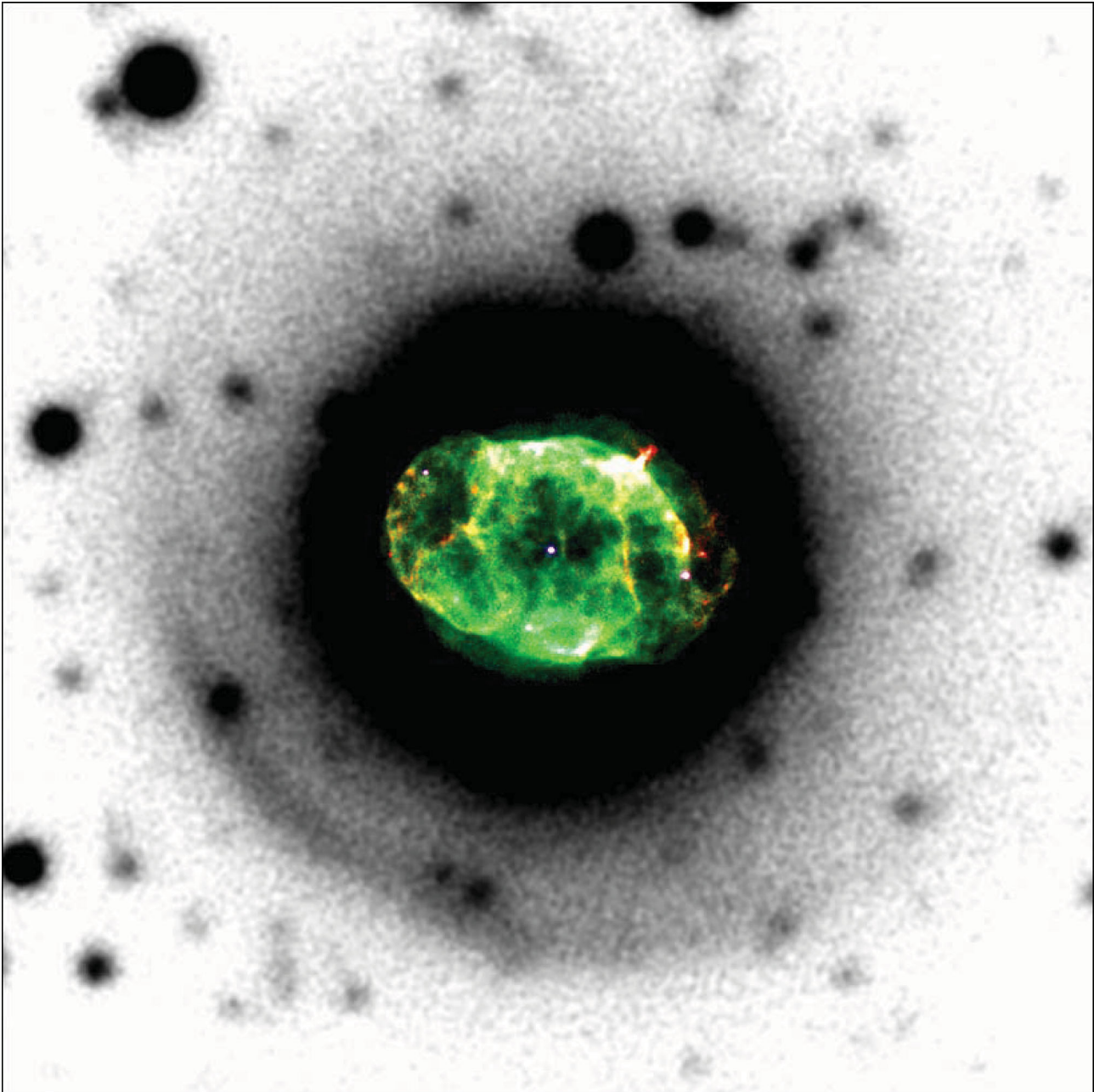


Figure 5. Gemini South GMOS [O III] image of IC 4663 (background) showing the newly discovered AGB halo, overlaid with an *HST* colour-composite image (red, green and blue channels were made from *F658N*, *F502N* and *F555W* images, respectively). The image is centred on the central star and measures $60 \times 60 \text{ arcsec}^2$ ($\sim 1 \text{ pc}$ across at 3.5 kpc) with north up and east to the left.

Table 3. Basic nebula properties of IC 4663.

PN G	346.2–08.2	
RA	$17^{\text{h}}45^{\text{m}}28^{\text{s}}.6$	
Dec.	$-44^{\circ}54'17''$	
Nebula diameter	$16.0 \times 19.5 \text{ arcsec}^2$	This work
Halo dimensions	$52.5 \times 55.0 \text{ arcsec}^2$	This work
$\log F(\text{H}\beta)$	-11.44	Shaw & Kaler (1989)
v_{exp}	30 km s^{-1}	Hajian et al. (2007)
v_{hrv}	$-78 \pm 3 \text{ km s}^{-1}$	This work
t_{neb}	$\sim 4400 \text{ yr}$	This work
t_{halo}	$\sim 30\,500 \text{ yr}$	This work

4.2 Chemical abundances and plasma parameters

The nebular spectrum of IC 4663 was previously analysed by CCM10 using low-resolution ($\sim 6 \text{ \AA}$ FWHM) spectroscopy obtained with a 1.6-m telescope. Fig. 6 shows our combined nebular spectrum made from averaging both of the 2400 s GMOS exposures. We compared the measured emission line intensities in our deep GMOS spectrum with the observations of CCM10 and found a good correlation with the line fluxes for the stronger lines, but also a tendency for the weak line fluxes to be overestimated by CCM10. For instance, the He I lines at $\lambda\lambda 4471$ and 6678 are twice as bright as expected from the $\lambda 5876$ line, whereas all four lines in our spectrum are close to their theoretical ratios. Similarly, the fluxes of [Ar IV]

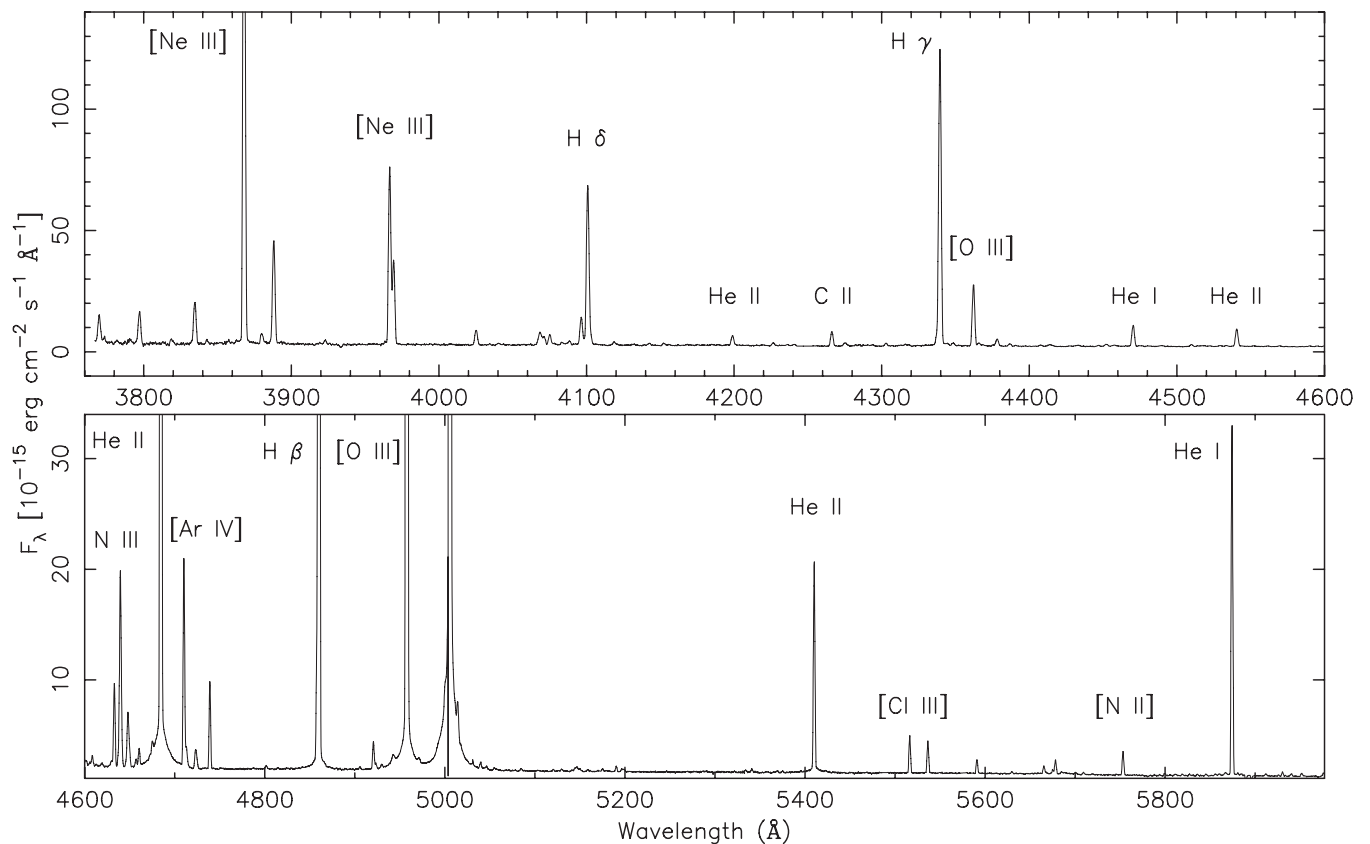


Figure 6. GMOS nebular spectrum of IC 4663 with the main lines identified. See Table 5 for line intensities.

$\lambda\lambda 7170$ and 7237 are ~ 3 times stronger than predicted from their $\lambda 4740$ line. Thus we shall ignore them in our analysis. Our [Ar IV] $\lambda 4740$ line is only 1/3 of the CCM10 value.

Since the GMOS spectrum is deeper with greater S/N we produced a composite spectrum by using line intensities from our deep GMOS spectrum for the blue part ($\lambda \leq 5900$ Å) and CCM10 for the red part (except for [O II] $\lambda 3728$ which lies outside our GMOS spectrum). The published intensities of CCM10 were reddened with the reddening law of Fitzpatrick (1999) for $R_V = 3.1$, and the fluxes were scaled to the GMOS $H\beta$ flux. We measured ultraviolet (UV) line fluxes from archival *IUE* spectra SWP33946 and LWP13707, observed on 1988 July 20, that were joined to the optical spectrum, taking into account the finite coverage of the *IUE* aperture. Although the aperture includes the central star, the low-dispersion *IUE* spectra only show nebula emission lines and no features from the central star. We estimate the stellar contribution to the *IUE* aperture at He II $\lambda 1640$ to be ~ 5 per cent in comparison with our *CMFGEN* model.

Tables 4 and 5 contain the full composite nebula spectrum of IC 4663. The line fluxes were analysed with the plasma diagnostics program *HOPPLA* (Acker et al. 1991; Köppen, Acker & Stenholm 1991; Girard, Köppen & Acker 2007) which first determines the extinction constant – using the $R_V = 3.1$ reddening law of Fitzpatrick (1999) – as well as the electron temperature and density in a consistent way. The $H\alpha/H\beta$ ratio would give $c = 0.58$, the inclusion of the blue Balmer lines gives a slightly smaller value of 0.54. We adopted $c = 0.51$ to be consistent with the dereddening of the stellar spectrum. In either case, all Balmer lines are fitted within 10 per cent of their intensity from case B recom-

Table 4. UV emission line intensities measured from the *IUE* spectra of IC 4633 (SWP33946 and LWP13707) scaled to $H\beta = 100$. Since the *IUE* aperture does not cover the entire nebula, the fluxes were scaled as to give the best agreement between the intensities of the UV and optical He II lines. The measured fluxes in units of 10^{-13} erg cm^{-2} s^{-1} Å $^{-1}$ may be obtained by dividing the flux values by 5.5.

Line	Flux	Intensity
C IV 1550	<8	–
He II 1640	124	558
[N III] 1753	6:	27:
C III] 1908	36	179
[Ne IV] 2424	25	106
He II 2734	10	28
O III 2837*	8:	20:
O III 3047*	11	26
O III 3133*	76	162
He II 3204	20	41
O III 3299*	18	36
O III 3341*	37	71

*Bowen fluorescence line.

bination theory. The He I line intensities are matched better than 10 per cent by case B recombination emissivities corrected for collisional excitation (Porter, Ferland & MacAdam 2007), except for the $\lambda\lambda 6678$ and 7065 lines from CCM10. We note that the choice of

Table 5. Nebular emission line intensities of IC 4663 scaled to $H\beta = 100$ as measured from our GMOS spectrum (first half) and CCM10 (second half). The CCM10 fluxes were obtained by reddenning the published intensities with $c = 0.58$ and the $R_V = 3.1$ law of Fitzpatrick (1999).

Line	Flux	Intensity
H I 3798	4.8	6.6
H I 3835	6.2	8.5
[Ne III] 3869	79.4	106.8
He I 3889	15.4	20.6
He II 3924	0.7	0.9
[Ne III]+H I 3967	24.6	32.1
H I 3970	11.5	15.0
He I 4026	2.3	3.0
[S II] 4068	2.8	3.6
O II 4072	1.5	1.9
[S II] 4076	1.5	1.9
N III 4097	4.2	5.2
H δ 4102	24.2	30.5
O II 4119	0.7	0.8
He II 4200	1.4	1.7
C II 4267	2.1	2.5
H γ 4340	43.9	51.5
[O III] 4363	8.8	10.3
N III 4379	1.2	1.3
He I 4388	0.45	0.4
He I 4472	3.1	3.5
N III 4511	2.5	2.8
N III 4634	2.8	3.0
N III 4641	7.3	7.8
O II 4649	2.5	2.6
He II 4686	80.6	85.3
[Ar IV]+He I 4711	6.9	7.0
[Ne IV] 4714	0.8	0.8
[Ne IV] 4724	0.9	0.9
[Ar IV] 4740	2.7	2.8
H β 4861	100.0	100.0
He I 4922	0.9	0.9
[O III] 4959	375.4	364.0
He II 5412	6.5	5.5
[Cl III] 5518	1.2	1.0
[Cl III] 5538	1.0	0.8
O III 5592	0.4	0.4
N II 5667	0.3	0.2
N II 5680	0.5	0.4
[N II] 5754	0.8	0.6
He I 5876	11.8	9.0
[O II] 3728	38.9	54.6
[O III] 5007	1085.0	1035.1
[S III] 6312	3.9	2.7
[Ar V] 6435	0.8	0.5
[N II] 6548	31.3	20.8
H α 6563	454.2	301.5
[N II] 6583	50.1	33.5
He I 6678	5.2	3.4
[S II] 6716	3.9	2.6
[S II] 6731	4.9	3.2
[Ar V] 7006	1.9	1.2
He I 7065	2.5	1.5
[Ar III] 7136	50.9	30.8
[Ar IV] 7170	2.1	1.3
[Ar IV] 7237	2.0	1.1
[O II] 7325	5.1	3.0
[Ar III] 7751	11.9	6.6

Table 6. Ionic abundances (relative to H^+) and the emission lines from which they were derived.

Ion	Ionic abundance	Lines used (\AA)
He ⁺	6.43×10^{-2}	5876, 4471, 6678, 7065, 4922, 4388
He ⁺⁺	6.58×10^{-2}	1640, 4686, 3203, 2734, 5411, 4199, 3923
C ⁺⁺	1.57×10^{-4}	1908
N ⁺	6.42×10^{-6}	6583, 6548, 5755
N ⁺⁺	1.22×10^{-4}	1753
O ⁺	1.79×10^{-5}	3728, 7325
O ⁺⁺	2.32×10^{-4}	5007, 4959, 4363
Ne ⁺⁺	5.92×10^{-5}	3869
Ne ³⁺	8.73×10^{-5}	2424, 4714, 4724
S ⁺	5.02×10^{-7}	4076, 4068, 6717, 6731
S ⁺⁺	4.78×10^{-6}	6312
Cl ⁺⁺	7.66×10^{-8}	5517, 5537
Ar ⁺⁺	1.96×10^{-6}	7135, 7750
Ar ³⁺	3.38×10^{-7}	4740
Ar ⁴⁺	1.42×10^{-7}	7005, 6434

Table 7. Plasma diagnostics and the chemical composition of IC 4663, given in the usual notation $12 + \log [n(X)/n(H)]$, from this work and from CCM10. For comparison the average abundances for Type I and non-Type I PNe are taken from Kingsburgh & Barlow (1994) and solar abundances from Asplund et al. (2009).

	IC 4663		Type I	Non-Type I	Sun
	This work	CCM10			
c	0.51	0.58	–	–	–
n_e (cm^{-3})	1000	3810	–	–	–
$T_e(\text{O}^+)$ (K)	10 300	12800	–	–	–
$T_e(\text{O}^{++})$ (K)	11 500	11500	–	–	–
$T_e(\text{He}^{++})$ (K)	11400	–	–	–	–
He	11.11	11.07	11.11	11.05	10.93
C	8.20	–	8.43	8.81	8.43
N	8.26	8.49	8.72	8.14	7.83
O	8.70	8.84	8.65	8.69	8.69
Ne	8.11	8.25	8.09	8.10	7.93
S	7.02	7.03	6.91	6.91	7.12
Cl	5.50	–	–	–	5.50
Ar	6.43	6.87	6.42	6.38	6.40
$\log(\text{C}/\text{O})$	–0.50	–	–0.12	+0.12	–0.26
$\log(\text{N}/\text{O})$	–0.45	–0.35	+0.07	–0.55	–0.86
$\log(\text{Ne}/\text{O})$	–0.59	–0.59	–0.56	–0.59	–0.76
$\log(\text{S}/\text{O})$	–1.68	–1.81	–1.74	–1.78	–1.57
$\log(\text{Cl}/\text{O})$	–3.20	–	–	–	–3.19
$\log(\text{Ar}/\text{O})$	–2.27	–1.97	–2.23	–2.31	–2.29

extinction constant has only very little influence on the derived elemental abundances (<0.04 dex).

With the adopted extinction, we then determined the aperture factor for the *IUE* spectrum by minimizing the error in the He II UV and optical lines $\lambda\lambda 1640, 4686$ and 3203 , according to case B recombination theory. This scaling factor is also consistent with the ratio of the nebular area and the *IUE* aperture (an ellipse measuring 10×20 arcsec²).

Ionic abundances were derived from each of the dereddened line intensities, listed in Table 6, using the electron temperatures for the low, middle and high ionic species (given in Table 7), and weighted with the emissivity of each line. Elemental abundances were obtained by summing over the ionic abundances and correcting

for unobserved stages of ionization:

$$\frac{\text{He}}{\text{H}} = \frac{\text{He}^+}{\text{H}^+} + \frac{\text{He}^{++}}{\text{H}^+}.$$

Carbon is derived solely from the C III] emission line (see below):

$$\frac{\text{C}}{\text{H}} = \frac{\text{C}^{++}}{\text{H}^+}.$$

We use the standard correction factors (e.g. Aller 1984):

$$\frac{\text{N}}{\text{H}} = \frac{\text{N}^+}{\text{H}^+} \frac{\text{O}/\text{H}}{\text{O}^{++}/\text{H}^+},$$

$$\frac{\text{O}}{\text{H}} = \left(\frac{\text{O}^+}{\text{H}^+} + \frac{\text{O}^{++}}{\text{H}^+} \right) \frac{\text{He}/\text{H}}{\text{He}^{++}/\text{H}^+}.$$

For neon, we use

$$\frac{\text{Ne}}{\text{H}} = \frac{\text{Ne}^{++}}{\text{H}^+} \frac{\text{O}/\text{H}}{\text{O}^{++}/\text{H}^+},$$

and note that the sum of Ne^{++} and Ne^{3+} gives only a slightly higher abundance of $12 + \log(\text{Ne}/\text{H}) = 8.17$. For sulphur and chlorine, we employ the ionization correction factors derived from photoionization models (Köppen et al. 1991):

$$\frac{\text{S}}{\text{H}} = \left(\frac{\text{S}^+}{\text{H}^+} + \frac{\text{S}^{++}}{\text{H}^+} \right) \left[1.43 + 0.196 \left(\frac{\text{O}^{++}}{\text{O}^+} \right)^{1.29} \right],$$

$$\frac{\text{Cl}}{\text{H}} = \frac{\text{Cl}^{++}}{\text{H}^+} \left(\frac{\text{He}/\text{H}}{\text{He}^{++}/\text{H}^+} \right)^2.$$

Argon is treated by the correction from Barker (1980):

$$\frac{\text{Ar}}{\text{H}} = \left(\frac{\text{Ar}^{++}}{\text{H}^+} + \frac{\text{Ar}^{3+}}{\text{H}^+} + \frac{\text{Ar}^{4+}}{\text{H}^+} \right) \frac{\text{S}^+ + \text{S}^{++}}{\text{S}^{++}}.$$

The resulting abundances are collated in Table 7. A few remarks are necessary. Our helium abundance is slightly higher than that found by CCM10. This is due to the intensity of the $\text{He I } \lambda 5876$ line being larger – by a factor of 1.4 – in our GMOS spectrum. Due to the ionization corrections this also results in lower oxygen and neon abundances. The intensity ratio of [N II] 6583/6548 (from CCM10) of 1.6 is substantially lower than the theoretical ratio of 2.9, which indicates problems with the separation of the lines from $\text{H}\alpha$. As to make use of all information, we use both lines, and we use the $\lambda 5755$ line from the GMOS spectrum. These choices influence our results on nitrogen, albeit not in a critical way. Taking the $\lambda 6583$ line only increases the electron temperature in the O^+ zone to 11 200 K, giving a slightly lower nitrogen abundance of 8.22, and $\text{N}/\text{O} = -0.48$. If we took also the $\lambda 5755$ intensity from CCM10 – which is larger by a factor of 1.5 than the GMOS value – the electron temperature increases further to 13 900 K, the nitrogen abundance to 8.27, and $\text{N}/\text{O} = -0.35$, the same value as derived by CCM10. Furthermore, from the just discernible [N III] $\lambda 1753$ line in the *IUE* spectrum, we may derive an ionic abundance which is substantially larger than that from N^+ . Since in a high excitation nebula nitrogen is found predominantly in the form of N^{++} , the derived nitrogen abundance of $12 + \log(\text{N}/\text{H}) = 8.11$ is a little less than that obtained from the [N II] lines, but with a substantial ionization correction factor (30–60 in the various cases considered here). This gives $\text{N}/\text{O} = -0.59$. We conclude that the nitrogen abundance is certainly in the range of 8.1–8.3, hence $\text{N}/\text{O} = -0.6$ to -0.3 . This is just below the threshold value for a bona fide Type I PN in Peimbert’s classification and well below the (linear) value of 0.8 for a Type I in the sense of Kingsburgh & Barlow (1994).

The C^{++} abundance derived from the optical recombination line at 4267 Å is about 30 times higher than that from the collisionally excited doublet C III] 1908 Å. This abundance discrepancy factor is larger than the usual factor of 2–3, but other extreme examples are known (e.g. Liu et al. 2006). The presence of N III and O III recombination lines is in agreement with the very high level of nebular excitation, which is in concordance with the UV flux distribution predicted from our model atmosphere for the central star. A recombination line analysis of the nebula spectrum will not be performed here.

Despite the high nebular excitation the *IUE* spectrum shows no detectable C IV $\lambda 1550$ emission. In nebulae with a large central hole, this line is strongly weakened, as the C^{3+} zone is remote from the central star, and hence the ionizing radiation is geometrically strongly diluted (cf. Köppen 1983). The monochromatic images of IC 4663 indeed suggest a bubble-type geometry for the emission region. Tests with photoionization models indicate that in a thin-shell type nebula the C IV lines can be suppressed sufficiently to agree with the *IUE* spectrum. As a consequence, we may assume that the C^{++} zone nearly completely fills the nebula, and that the carbon abundance derived from the C III] 1908 lines may be close to the true value. Since the nebula has a rather elliptical shape and also shows indications for a double shell, we refrain from constructing a spherical photoionization model.

The derived abundances show that our He/H is slightly higher than that in CCM10 and closer to a Type I composition (Peimbert & Torres-Peimbert 1983; Kingsburgh & Barlow 1994), because the $\text{He I } 5876$ intensity from the GMOS spectrum is higher. We note that our value is also consistent with the other He I lines. However, the N/O ratio is not as high as to classify it as a genuine Type I nebula. The nearly solar oxygen abundance is also similar to the average PN, as are the Ne/O and S/O ratios. The ratios of the α elements are close to the average values found in H II regions of spiral and irregular galaxies (Henry & Worthey 1999), namely $\text{Ne}/\text{O} = -0.67$ (slightly lower than in PN and in IC 4663), $\text{S}/\text{O} = -1.55$ (slightly higher than that in IC 4663) and $\text{Ar}/\text{O} = -2.25$. Since these elements are not expected to be affected by nucleosynthesis in the progenitor star, their ratios reflect the ISM values which are determined by nucleosynthesis in massive stars.

The carbon-to-oxygen ratio is lower than in both PN types and the Sun, but in light of both the strong sensitivity of the UV lines to electron temperature and the uncertainty of the ionization correction factor for carbon, this difference of 0.3 dex cannot be taken as a solid proof for a carbon underabundance. If placed in fig. 7 of Henry & Worthey (1999), IC 4663 would be located near the lower envelope of scattered points, but would still be consistent with the average relation. Finally, the chlorine-to-oxygen ratio is solar. The abundance pattern of IC 4663 is close to the Sun, except for enhancements in helium, nitrogen and neon.

4.3 Evolutionary status

The evolutionary state of the PN IC 4663 may also be compared against other PNe using the distance-independent parameters $\log S_V$ and $\log S_{H\beta}$ (Górny & Tylenda 2000). The parameters are defined as the $H\beta$ surface brightness and an analogous quantity replacing $F_{H\beta}$ with F_V , an extinction-corrected stellar flux in the *V* band, respectively. Both S_V and $S_{H\beta}$ decrease as a PN expands and evolves towards the WD state. Fig. 7 portrays the position of IC 4663 amongst other PNe with H-deficient central stars ($\log S_V = -6.54$ and $\log S_{H\beta} = -2.71$) and PB 8 ($\log S_V = -4.11$ and $\log S_{H\beta} = -1.48$, based on the updated parameters in Todt et al. 2010a). The

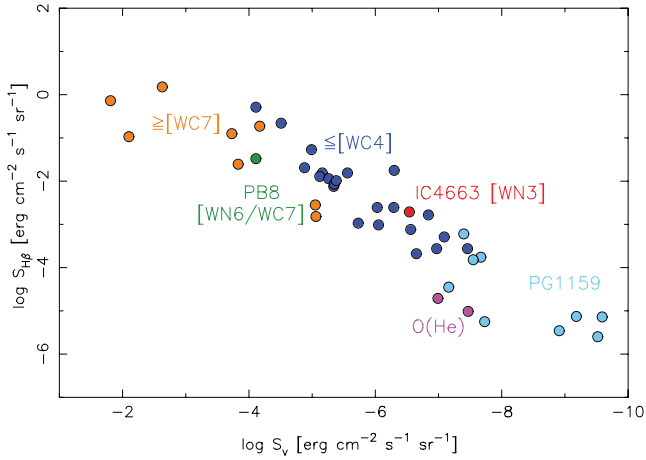


Figure 7. Hydrogen-deficient PNe in the distance-independent $\log S_V$ and $\log S_{H\beta}$ plane (see Górný & Tylenda 2000).

location of IC 4663 is coincident with PNe that have a [WO] central star (i.e. [WC4] or earlier) and PB 8 with those that have a [WC] central star (i.e. [WC7] or later).

5 DISCUSSION

5.1 A bona fide PN

Table 8 delineates three illustrative distance scenarios for IC 4663. At an assumed distance of 3.5 kpc (SSV08), the central star has $M_V = +3.1$ mag. This is over 6 mag fainter than $M_V = -3.0$ mag, the typical luminosity for a massive WN3 star (Crowther et al. 1995a; Hamann et al. 2006). The other two scenarios demonstrate that the subluminal nature of the central star is robust against any reasonable uncertainties that may be associated with the distance of SSV08. Even if IC 4663 were a member of the Galactic Bulge at $d = 8.0$ kpc, then the central star is still at least 4 mag too faint. IC 4663 cannot however be a member of the Bulge because its angular diameter and $H\beta$ flux are anomalously large compared to most Bulge PNe (see fig. 7 of Górný et al. 2009). Indeed, an implausible distance of 58 kpc would be required to reproduce $M_V = -3.0$ mag; therefore, for any reasonable distance estimate the central star must be subluminal and belong to the PN. At 3.5 kpc IC 4663 would lie 500 pc below the Galactic Plane, i.e. between the bias-corrected scale heights of the thin (300–375 pc) and thick (900–940 pc) discs (Siegel et al. 2002; Jurić et al. 2008). Massive WR stars that are not runaway stars would be restricted to the young disc population which has a scale height of only $\sim 48 \pm 3$ pc (Bonatto et al. 2006). This intermediate height might on its own suggest a thick disc progenitor; however, the solar oxygen and argon abundances, which

Table 8. Absolute visual magnitudes and vertical displacement from Galactic Plane for the central star of IC 4663 at a range of distances [$V = 16.90$ mag and $E(B - V) = 0.35$ mag, Section 4.1].

d (kpc)	M_V	z (kpc)	Comment
3.5	+3.1	-0.50	d from SSV08
8.0	+1.3	-1.14	d of Galactic Bulge PN
58.0	-3.0	-8.27	M_V of massive WN3 star

reflect the metallicity of the gas which formed the progenitor star, suggest that IC 4663 is a thin disc object.

The presence of an AGB halo is a telltale signature of a PN (Corradi et al. 2003). The ellipsoidal morphology of the main nebula, its relatively low expansion velocity and density are all typical of PNe. Its evolutionary status overlaps with other PNe in Fig. 7 and exhibits a highly ionized emission-line spectrum with a typical chemical abundance pattern for a PN.

5.2 A second post-AGB H-deficient and He-rich evolutionary sequence

Table 9 contrasts the He-dominated composition of the [WN3] central star of IC 4663 against those of other H-deficient post-AGB stars.⁸ Clearly IC 4663 does not fit the carbon- and oxygen-rich evolutionary sequence [WCL] \rightarrow [WCE] \rightarrow PG 1159 (Werner & Herwig 2006). Rather, it fits amongst other rare He-dominated objects including RCB stars, O(He) stars, extreme helium B stars and helium-rich subdwarf O stars for which there is no accepted explanation for their origin (Werner & Herwig 2006). The born-again evolutionary models simply cannot reproduce the helium-dominated atmospheres (e.g. Herwig 2001). Some proposed explanations include a double-degenerate merger (Saio & Jeffery 2002), a low-mass star leaving the AGB shortly after the first thermal pulse (Miller Bertolami & Althaus 2006) or a diffusion-induced nova (Miller Bertolami et al. 2011).

If we speculate that IC 4663 has a companion, then perhaps a close binary evolution channel may be responsible for the helium-rich composition. Yungelson (2008) proposed such a scheme to explain helium-rich AM Canum Venaticorum (AM CVn) stars (Warner 1995; Solheim 2010). IC 4663 may be the ejected CE at one of these stages making it a possible AM CVn progenitor. If IC 4663 were a pre-CV, then it could potentially evolve into a helium-rich nova after additional angular momentum loss (e.g. V445 Puppis; Woudt et al. 2009). Another possibility is that a CE merger already took place and this would be consistent with the apparent lack of evidence for a close binary (Section 3.4). More generally this would help explain the apparent lack of [WR] central stars in close binaries, despite many nebulae around [WR] central stars showing post-CE morphologies (Miszalski et al. 2009b).

The discovery of the [WN3] central star of IC 4663 has several implications. Joining the O(He) stars (Méndez 1991; Rauch et al. 1994, 1996, 1998, 2008) it is now the fifth hot ($T_{\text{eff}} \gtrsim 100$ kK), He-rich and H-deficient post-AGB star known. A second post-AGB H-deficient sequence [WN] \rightarrow O(He) now seems to be a logical conclusion based on the strong match between their compositions. This has been hypothesized before (e.g. Werner 2012), but only now does it seem to be real with the [WN3] discovery in IC 4663. The RCB stars may also play an uncertain role in this sequence as RCB \rightarrow [WN] \rightarrow O(He). The nebula evolutionary status of IC 4663 and the two PNe with O(He) central stars (Section 4.3), being coincident with [WO] and PG 1159 stars, respectively, supports the existence of a second sequence as their evolutionary status mirrors the [WC] \rightarrow PG 1159 sequence. Once the stellar wind of the [WN3] central star of IC 4663 disappears it will likely become an O(He) central star and later a DO WD.

In summary, we propose that the [WN] \rightarrow O(He) sequence is a logical conclusion from the strong match between the surface

⁸ Some caution should be taken when comparing compositions derived from different analysis techniques (see e.g. Werner & Herwig 2006).

Table 9. Stellar compositions expressed as mass fractions (per cent) of IC 4663 and other objects with similar compositions.

Object	Type	T_{eff} (kK)	$\log g$ (CGS)	\dot{M} ($M_{\odot} \text{ yr}^{-1}$)	H	He	C	N	O	Ne	Reference
IC 4663	[WN3]	140	6.1 ^a	1.8×10^{-8}	<2	95	<0.1 ^b	0.8	0.05	0.2	This work
K 1-27	O(He)	105	6.5	7.9×10^{-10}	<5	98	<1.5	1.7	–	–	Rauch et al. (1998)
LoTr 4	O(He)	120	5.5	2.0×10^{-8}	11	89	<1	0.3	<3	–	Rauch et al. (1998)
PB 8	[WN6/WC7]	52	–	8.5×10^{-8}	40	55	1.3	2	1.3	–	Todt et al. (2010a)
RY Sgr	RCB	7.25	0.7	–	6×10^{-4}	98	0.7	0.3	0.09	–	Asplund et al. (2000)

^aAdopted value assuming $M = 0.6 M_{\odot}$.

^bModel constrained (no carbon lines observed).

compositions of the [WN3] central star of IC 4663 and the O(He) stars (Table 9). The evolutionary status of their nebulae (Section 4.3) suggests that it forms a second parallel H-deficient evolutionary sequence to the existing carbon-rich [WC] \rightarrow PG 1159 sequence. The relatively large amount of residual hydrogen in PB 8 suggests that it may belong to a separate [WN] sequence to IC 4663, perhaps reflecting the dichotomy between H-deficient early-type WN stars and H-rich late-type WN stars (e.g. Hamann et al. 2006).

6 CONCLUSIONS

We have discovered the first bona fide [WN] central star of a PN in IC 4663. Our main conclusions are as follows.

(i) The Gemini South GMOS spectrum of the central star is dominated by broad He II and N V emission lines, which, together with the notable absence of He I and C IV, corresponds to a [WN3] subtype.

(ii) A CMFGEN NLTE model atmosphere of the central star was built and reasonably reproduces the GMOS spectrum. The central star has a very hot ($T_* = 140$ kK) and fast ($v_{\infty} = 1900$ km s⁻¹) stellar wind. The atmosphere consists of helium (95 per cent), hydrogen (<2 per cent), nitrogen (0.8 per cent), neon (0.2 per cent) and oxygen (0.05 per cent) by mass. Such a composition cannot be explained by extant scenarios that seek to explain the H-deficiency of post-AGB stars.

(iii) The helium-rich atmospheric composition strongly links [WN] central stars to the O(He) central stars (Rauch et al. 1998). The data support a second post-AGB H-deficient evolutionary sequence [WN] \rightarrow O(He) parallel to the established carbon-rich [WCL] \rightarrow [WCE] \rightarrow PG 1159 sequence. Evolutionary connections to other He-rich/H-deficient stars may include RCB stars, and if there were a binary companion to the [WN3] star, AM CVn stars and He-rich novae after further angular momentum loss. The existence of this second sequence strongly suggests another mechanism exists for producing H-deficient post-AGB stars besides the various born-again scenarios.

(iv) For all reasonable distances the luminosity of the central star is 4–6 mag fainter than massive WN3 stars (Crowther et al. 1995a). At our assumed distance of 3.5 kpc (SSV08), the derived luminosity is $\log L/L_{\odot} = 3.6$, the stellar radius $R_* = 0.11 R_{\odot}$ and the mass-loss rate $\dot{M} = 1.8 \times 10^{-8} M_{\odot} \text{ yr}^{-1}$. The transformed radius, R_t , of $13.4 R_{\odot}$ for IC 4663 is comparable to massive WN3 stars, indicating a similar stellar wind density to its massive counterparts. This favours our morphological [WN3] classification of the central star of IC 4663, rather than alternative weak-wind (Of or Of-WR) classifications (Méndez et al. 1990; Méndez 1991).

(v) The surrounding nebula is a bona fide PN. The elliptical main nebula has a relatively low expansion velocity of 30 km s⁻¹ and is surrounded by a newly discovered AGB halo. The evolutionary

status of the highly ionized nebula corresponds to that of similar nebulae around [WO] type central stars and supports the [WN] \rightarrow O(He) evolutionary sequence.

(vi) Chemical abundances of the nebula were derived from a combination of IUE, GMOS and CCM10 emission line intensities. The abundance pattern is approximately solar with slight enhancements for helium, nitrogen and neon. The carbon-to-oxygen ratio is lower than in the Sun; however, the data are insufficient to prove a carbon underabundance.

(vii) We found no evidence for RV variability from the central star $\gtrsim 5$ –10 km s⁻¹ in three epochs. Further monitoring of the central star should be performed to conclusively rule out the presence of a companion to the [WN3] central star.

ACKNOWLEDGMENTS

We acknowledge the conscientious and helpful support of Michelle Edwards, Henry Lee and Andrew Gosling during the course of our Gemini programme. We thank Sławomir Górny for valuable help in calculating S_V and $S_{H\beta}$ and Joanna Mikołajewska for discussions on symbiotic novae. AFJM is grateful to NSERC (Canada) and FQRNT (Quebec) for financial assistance. This work was primarily based on observations obtained at the Gemini Observatory, which is operated by the Association of Universities for Research in Astronomy, Inc., under a cooperative agreement with the NSF on behalf of the Gemini partnership: the National Science Foundation (USA), the Science and Technology Facilities Council (UK), the National Research Council (Canada), CONICYT (Chile), the Australian Research Council (Australia), Ministério da Ciência e Tecnologia (Brazil) and Ministerio de Ciencia, Tecnología e Innovación Productiva (Argentina). It also used observations made with the NASA/ESA *Hubble Space Telescope*, and obtained from the Hubble Legacy Archive, which is a collaboration between the Space Telescope Science Institute (STScI/NASA), the Space Telescope European Coordinating Facility (ST-ECF/ESA) and the Canadian Astronomy Data Centre (CADAC/NRC/CSA). JK thanks the Institut für Theoretische Physik und Astrophysik der Universität zu Kiel for the hospitality during several visits.

REFERENCES

- Abell G. O., 1966, *ApJ*, 144, 259
 Acker A., Neiner C., 2003, *A&A*, 403, 659
 Acker A., Raytchev B., Köppen J., Stenholm B., 1991, *A&AS*, 89, 237
 Aller L. H., 1968, in Osterbrock D. E., O'Dell C. R., eds, *Proc. IAU Symp.* 34, Planetary Nebulae. Reidel, Dordrecht, p. 339
 Aller L. H., 1984, *Astrophysics and Space Science Library*, Vol. 112, Physics of Thermal Gaseous Nebulae. Reidel, Dordrecht
 Appenzeller I. et al., 1998, *The Messenger*, 94, 1

- Asplund M., Gustafsson B., Lambert D. L., Rao N. K., 2000, *A&A*, 353, 287
- Asplund M., Grevesse N., Sauval A. J., Scott P., 2009, *ARA&A*, 47, 481
- Barker T., 1980, *ApJ*, 240, 99
- Beaulieu S. F., Dopita M. A., Freeman K. C., 1999, *ApJ*, 515, 610
- Blöcker T., 2001, *Ap&SS*, 275, 1
- Bonatto C., Kerber L. O., Bica E., Santiago B. X., 2006, *A&A*, 446, 121
- Bond H. E., 2008, in Werner K., Rauch T., eds, *ASP Conf. Ser. Vol. 391, Hydrogen-Deficient Stars. Astron. Soc. Pac.*, San Francisco, p. 129
- Cavichia O., Costa R. D. D., Maciel W. J., 2010, *Rev. Mex. Astron. Astrofis.*, 46, 159 (CCM10)
- Chu Y.-H., 1982, *ApJ*, 254, 578
- Clayton G. C., 1996, *PASP*, 108, 225
- Clayton G. C., De Marco O., 1997, *AJ*, 114, 2679
- Clayton G. C., Kerber F., Pirzkal N., De Marco O., Crowther P. A., Fedrow J. M., 2006, *ApJ*, 646, L69
- Clayton G. C., Geballe T. R., Herwig F., Fryer C., Asplund M., 2007, *ApJ*, 662, 1220
- Clayton G. C. et al., 2011a, *AJ*, 142, 54
- Clayton G. C. et al., 2011b, *ApJ*, 743, 44
- Corradi R. L. M., Schönberner D., Steffen M., Perinotto M., 2003, *MNRAS*, 340, 417
- Crawford I. A., Barlow M. J., 1991a, *A&A*, 249, 518
- Crawford I. A., Barlow M. J., 1991b, *A&A*, 251, L39
- Crowther P. A., 2008, in Werner K., Rauch T., eds, *ASP Conf. Ser. Vol. 391, Hydrogen-Deficient Stars. Astron. Soc. Pac.*, San Francisco, p. 83
- Crowther P. A., Smith L. J., Hillier D. J., 1995a, *A&A*, 302, 457
- Crowther P. A., Smith L. J., 1995b, *A&A*, 304, 269
- Crowther P. A., De Marco O., Barlow M. J., 1998, *MNRAS*, 296, 367
- Crowther P. A., Morris P. W., Smith J. D., 2006, *ApJ*, 636, 1033
- De Marco O., 2008, in Werner K., Rauch T., eds, *ASP Conf. Ser. Vol. 391, Hydrogen-Deficient Stars. Astron. Soc. Pac.*, San Francisco, p. 209
- De Marco O., Soker N., 2002, *PASP*, 114, 602
- DePew K., Parker Q. A., Miszalski B., De Marco O., Frew D. J., Acker A., Kovacevic A. V., Sharp R. G., 2011, *MNRAS*, 414, 2812
- Drew J. E. et al., 2005, *MNRAS*, 362, 753
- Duerbeck H. W., Reipurth B., 1990, *A&A*, 231, L11
- Fitzpatrick E. L., 1999, *PASP*, 111, 63
- Fleming W., Pickering E. C., 1910, *Harvard College Observ. Circ.*, 158, 1
- Girard P., Köppen J., Acker A., 2007, *A&A*, 463, 265
- González-Solares E. A. et al., 2008, *MNRAS*, 388, 89
- Gonçalves D. R., Corradi R. L. M., Mampaso A., 2001, *ApJ*, 547, 302
- Górny S. K., Tylenda R., 2000, *A&A*, 362, 1008
- Górny S. K., Stasińska G., Escudero A. V., Costa R. D. D., 2004, *A&A*, 427, 231
- Górny S. K., Chiappini C., Stasińska G., Cuisinier F., 2009, *A&A*, 500, 1089
- Górny S. K., Perea-Caldern J. V., García-Hernández D. A., García-Lario P., Szczerba R., 2010, *A&A*, 516, A39
- Grosdidier Y., Acker A., Moffat A. F. J., 2000, *A&A*, 364, 597
- Grosdidier Y., Moffat A. F. J., Blais-Ouellette S., Joncas G., Acker A., 2001a, *ApJ*, 562, 753
- Grosdidier Y., Acker A., Moffat A. F. J., 2001b, *A&A*, 370, 513
- Hajduk M., Zijlstra A. A., Gesicki K., 2010, *MNRAS*, 406, 626
- Hajian A. R. et al., 2007, *ApJS*, 169, 289
- Hamann W.-R., Koesterke L., Wessolowski U., 1995, *A&AS*, 113, 459
- Hamann W.-R., Peña M., Gräfener G., Ruiz M. T., 2003, *A&A*, 409, 969
- Hamann W.-R., Gräfener G., Liermann A., 2006, *A&A*, 457, 1015
- Hambly N. C. et al., 2001, *MNRAS*, 326, 1279
- Henry R. B. C., Worthey G., 1999, *PASP*, 111, 919
- Herwig F., 2001, *Ap&SS*, 275, 15
- Hillier D. J., Miller D. L., 1998, *ApJ*, 496, 407
- Hook I. M., Jørgensen I., Allington-Smith J. R., Davies R. L., Metcalfe N., Murowinski R. G., Crampton D., 2004, *PASP*, 116, 425
- Howarth I. D., 1983, *MNRAS*, 203, 301
- Hubeny I., Lanz T., 1995, *ApJ*, 439, 875
- Jurić M. et al., 2008, *ApJ*, 673, 84
- Kingsburgh R. L., Barlow M. J., 1994, *MNRAS*, 271, 257
- Koesterke L., Hamann W.-R., 1997, *A&A*, 320, 91
- Köppen J., 1983, *A&A*, 122, 95
- Köppen J., Acker A., Stenholm B., 1991, *A&A*, 248, 197
- Lau H. H. B., De Marco O., Liu X.-W., 2011, *MNRAS*, 410, 1870
- Lépine S., Moffat A. F. J., 1999, *ApJ*, 514, 909
- Liu X.-W., Barlow M. J., Zhang Y., Bastin R. J., Storey P. J., 2006, *MNRAS*, 368, 1959
- Lopez J. A., Meaburn J., Palmer J. W., 1993, *ApJ*, 415, L135
- Marchenko S. V., Moffat A. F. J., Crowther P. A., 2010, *ApJ*, 724, L90
- Massey P., Grove K., 1989, *ApJ*, 344, 870
- Méndez R. H., 1991, in Michaud G., Tutukov A. V., eds, *Proc. IAU Symp. 145, Evolution of Stars: the Photospheric Abundance Connection*. Kluwer, Dordrecht, p. 375
- Méndez R. H., Herrero A., Manchado A., 1990, *A&A*, 229, 152
- Miller Bertolami M. M., Althaus L. G., 2006, *A&A*, 454, 845
- Miller Bertolami M. M., Althaus L. G., Olano C., Jiménez N., 2011, *MNRAS*, 415, 1396
- Miszalski B., Acker A., Moffat A. F. J., Parker Q. A., Udalski A., 2009a, *A&A*, 496, 813
- Miszalski B., Acker A., Parker Q. A., Moffat A. F. J., 2009b, *A&A*, 505, 249
- Miszalski B., Jones D., Rodríguez-Gil P., Boffin H. M. J., Corradi R. L. M., Santander-García M., 2011a, *A&A*, 531, A158
- Miszalski B., Corradi R. L. M., Jones D., Santander-García M., Rodríguez-Gil P., Rubio-Díez M. M., 2011b, in Zijlstra A. A., Lykou F., McDonald I., Lagadec E., eds, *Asymmetric Planetary Nebulae 5 Conference*. Jordrell Bank Centre for Astrophysics, UK
- Moffat A. F. J., 1996, *Liege Int. Astrophys. Colloq.*, 33, 199
- Morgan D. H., Parker Q. A., Russeil D., 2001, *MNRAS*, 322, 877
- Morgan D. H., Parker Q. A., Cohen M., 2003, *MNRAS*, 346, 719
- Napiwotzki R., Schönberner D., 1995, *A&A*, 301, 545
- Nussbaumer H., 1996, *Ap&SS*, 238, 125
- Parker Q. A., Morgan D. H., 2003, *MNRAS*, 341, 961
- Parker Q. A. et al., 2005, *MNRAS*, 362, 689
- Peimbert M., Torres-Peimbert S., 1983, in Flower D. R., ed., *Proc. IAU Symp. 103, Planetary Nebulae*. Reidel, Dordrecht, p. 233
- Peña M., Torres-Peimbert S., Peimbert M., Ruiz M. T., Maza J., 1994, *ApJ*, 428, L9
- Peña M., Hamann W.-R., Koesterke L., Maza J., Mendez R. H., Peimbert M., Ruiz M. T., Torres-Peimbert S., 1997, *ApJ*, 491, 233
- Peña M., Hamann W.-R., Ruiz M. T., Peimbert A., Peimbert M., 2004, *A&A*, 419, 583
- Peña M., Ruiz M. T., Rojo P., Torres-Peimbert S., Hamann W.-R., 2008, *ApJ*, 680, L109
- Perek L., Kohoutek L., 1967, *Catalogue of galactic planetary nebulae*. Publication House of the Czechoslovak Academy of Sciences, Prague
- Porter R. L., Ferland G. J., MacAdam K. B., 2007, *ApJ*, 657, 327
- Rauch T., Köppen J., Werner K., 1994, *A&A*, 286, 543
- Rauch T., Köppen J., Werner K., 1996, *A&A*, 310, 613
- Rauch T., Dreizler S., Wolff B., 1998, *A&A*, 338, 651
- Rauch T., Reiff E., Werner K., Kruk J. W., 2008, in Werner K., Rauch T., eds, *ASP Conf. Ser. Vol. 391, Hydrogen-Deficient Stars. Astron. Soc. Pac.*, San Francisco, p. 135
- Saio H., Jeffery C. S., 2002, *MNRAS*, 333, 121
- Schönberner D., 1979, *A&A*, 79, 108
- Schönberner D., 2008, in Werner K., Rauch T., eds, *ASP Conf. Ser. Vol. 391, Hydrogen-Deficient Stars. Astron. Soc. Pac.*, San Francisco, p. 139
- Shaw R. A., Kaler J. B., 1989, *ApJS*, 69, 495
- Siegel M. H., Majewski S. R., Reid I. N., Thompson I. B., 2002, *ApJ*, 578, 151
- Smith L. F., Maeder A., 1991, *A&A*, 241, 77
- Smith L. F., Shara M. M., Moffat A. F. J., 1996, *MNRAS*, 281, 163
- Solheim J.-E., 2010, *PASP*, 122, 1133
- Stanghellini L., Shaw R. A., Villaver E., 2008, *ApJ*, 689, 194 (SSV08)
- Stock D. J., Barlow M. J., 2010, *MNRAS*, 409, 1429
- Thackeray A. D., Webster B. L., 1974, *MNRAS*, 168, 101
- Todt H., Peña M., Hamann W.-R., Gräfener G., 2008, in Werner K., Rauch T., eds, *ASP Conf. Ser. Vol. 391, Hydrogen-Deficient Stars. Astron. Soc. Pac.*, San Francisco, p. 95

- Todt H., Peña M., Hamann W.-R., Gräfenor G., 2010a, *A&A*, 515, A83
- Todt H., Peña M., Hamann W.-R., Gräfenor G., 2010b, in Werner K., Rauch T., eds, *AIP Conf. Ser. Vol. 1273*, 17th European White Dwarf Workshop. Am. Inst. Phys., New York, p. 219
- Tylenda R., Acker A., Raytchev B., Stenholm B., Gleizes F., 1991, *A&AS*, 89, 77
- van der Hucht K. A., 2001, *New Astron. Rev.*, 45, 135
- Wachter S., Mauerhan J. C., Van Dyk S. D., Hoard D. W., Kafka S., Morris P. W., 2010, *AJ*, 139, 2330
- Wang W., Liu X.-W., 2008, *MNRAS*, 389, L33
- Warner B., 1995, *Ap&SS*, 225, 249
- Wendker H. J., Smith L. F., Israel F. P., Habing H. J., Dickel H. R., 1975, *A&A*, 42, 173
- Werner K., 2012, in *Proc. IAU Symp. 283*, in press preprint (arXiv:1109.2391)
- Werner K., Herwig F., 2006, *PASP*, 118, 183
- Werner K., Rauch T., Kruk J. W., 2007, *A&A*, 474, 591
- Wesemael F., Green R. F., Liebert J., 1985, *ApJS*, 58, 379
- Wesson R., Liu X.-W., Barlow M. J., 2003, *MNRAS*, 340, 253
- Wesson R., Barlow M. J., Liu X.-W., Storey P. J., Ercolano B., De Marco O., 2008, *MNRAS*, 383, 1639
- Woudt P. A. et al., 2009, *ApJ*, 706, 738
- Yungelson L. R., 2008, *Astron. Lett.*, 34, 620

This paper has been typeset from a $\text{\TeX}/\text{\LaTeX}$ file prepared by the author.